ResearchGate

See discussions, stats, and author profiles for this publication at: https://www.researchgate.net/publication/14633596

Kressin K, Kuprijanova E, Jabs R, Seifert G, Steinhauser C.. Developmental regulation of Na+ and K+ conductances in glial cells of mouse hippocampal brain slices. Glia 15: 173–187

ARTICLE *in* GLIA · OCTOBER 1995

Impact Factor: 6.03 · DOI: 10.1002/glia.440150210 · Source: PubMed

CITATIONS
115

READS
23

5 AUTHORS, INCLUDING:

Ronald Jabs
University of Bonn
26 PUBLICATIONS **1,237** CITATIONS
SEE PROFILE

Gerald Seifert
University of Bonn
80 PUBLICATIONS **3,724** CITATIONS
SEE PROFILE

Available from: Ronald Jabs
Retrieved on: 25 January 2016

GLIA 15:173–187 (1995)

Developmental Regulation of Na^+ and K^+ Conductances in Glial Cells of Mouse Hippocampal Brain Slices

KLAUS KRESSIN, ELENA KUPRIJANOVA, RONALD JABS, GERALD SEIFERT, AND CHRISTIAN STEINHÄUSER
Institute of Physiology, Friedrich-Schiller University Jena, 07740 Jena, Germany

KEY WORDS Astrocyte, Patch-clamp, Potassium channels, Sodium channels, Electrophysiology

ABSTRACT The relative contribution of voltage activated Na^+ and K^+ currents to the whole cell current pattern of hippocampal glial cells was analyzed and compared during different stages of postnatal maturation. The patch-clamp technique was applied to identified cells in thin brain slices obtained from animals between postnatal day 5 and 35 (p5–35). We focused on a subpopulation of glial cells in the CA1 stratum radiatum which most probably represents a pool of immature astrocytes, termed "complex" cells. These cells could not be labelled by O1/O4 antibodies, but some of the older cells were positively stained for glial fibrillary acidic protein (GFAP). In the early postnatal days, the current pattern of the "complex" cells was dominated by two types of K^+ outward currents: a delayed rectifier and a transient component. In addition, all cells expressed significant tetrodotoxin (TTX)-sensitive Na^+ currents. During maturation, the contribution of delayed rectifier and A-type currents significantly decreased. Furthermore, almost all cells after p20 lacked Na^+ currents. This down-regulation of voltage gated Na^+ and K^+ outward currents was accompanied by a substantial increase in passive and inward rectifier K^+ conductances. We found increasing evidence of electrical coupling between the "complex" cells with continued development. It is concluded that these developmental changes in the electrophysiological properties of "complex" glial cells could be jointly responsible for the well known impaired K^+ homeostasis in the early postnatal hippocampus. © 1995 Wiley-Liss, Inc.

INTRODUCTION

There is a large body of evidence supporting a developmental change in the electrophysiological properties in many neuronal cell types. Several studies have demonstrated that the sequence of ion channel expression during development is specific for a given cell type (reviewed by Spitzer, 1991), and various reports demonstrated changes in the expression pattern of ion channels with maturation in cultured glial cells (Barres, 1990; Blankenfeld et al., 1992; Borges et al., 1994; Sontheimer et al., 1989, 1991a,b, 1992). It is now well established that the expression of voltage-operated ion channels is not restricted to neurons, but also characterizes different glial cell types in situ (Berger et al., 1991, 1992; Clark and Mobbs, 1994; Müller et al., 1994; Sontheimer and Waxman, 1993; Steinhäuser et al., 1992, 1994b; Tse et al., 1992; see reviews by Ritchie, 1992, Sontheimer, 1994 or Steinhäuser, 1993). Glial cells in grey matter of the CNS can be distinguished according to their distinct electrophysiological properties. A previous study performed in the CA1 stratum radiatum of thin hippocampal brain slices at postnatal days (p) 10–12 revealed a heterogeneity of glial cells with respect to their electrophysiological properties (Steinhäuser et al.,

© 1995 Wiley-Liss, Inc.

Received May 17, 1995; accepted May 17, 1995.

R. Jabs is now at the Department of Physiology, College of Medicine, University of Saskatchewan, Saskatoon, Canada, S7N 0W0.

Address reprint requests to Dr. Christian Steinhäuser, Institute of Physiology, University of Jena, Teichgraben 8, 07740 Jena, Germany.

1992). These cells were unequivocally identified as glial by ultrastructural characterization.

Glial cells are thought to play an important role in the regulation of K^+ homeostasis (Orkand et al., 1966; Walz, 1989). There are different reports demonstrating an impaired K^+ homeostasis in the developing CNS, and it was supposed that the enhanced level of rises in $[K^+]_o$ observed during the first postnatal weeks reflects incomplete gliogenesis or insufficient glial cell function (Hablitz and Heinemann, 1987; Jendelova and Sykova, 1991; Lehmenkühler et al., 1993). A recent morphological study by Nixdorf-Bergweiler et al. (1994) suggested that changes in number, size, and orientation of astrocytes may contribute to the delayed maturation of K^+ homeostasis in the rat hippocampus, an area which is highly sensitive to the development of seizures or epileptiform activity. In the present study, we addressed the question whether changes in the electrophysiological properties of glial cells during this critical period could also contribute to these phenomena. The properties of hippocampal glial cells were recently studied in rat brain slices between p5 and p25 (Sontheimer and Waxman, 1993). This study provided an overview on qualitative variations in the current pattern of oligodendrocytes and astrocytes in various hippocampal subareas. We were interested in a quantitative measure of developmental changes in current expression of a given glial cell type. To restrict cellular heterogeneity (Patel, 1986; Wilkin et al., 1990), the patch-clamp technique was applied to identified cells located in a defined region of the hippocampus, namely the stratum radiatum of the CA1 region. We focused on "complex" cells which expressed voltage gated Na^+ currents and four types of K^+ currents; they represent a population of immature astrocytes. The relative contribution of the ionic conductances expressed in these cells was calculated and compared between postnatal days 5 and 35.

Some results of this study have been reported previously in abstract form (Kressin et al., 1994).

MATERIALS AND METHODS

Female mice (p5–35) were ether anaesthetized, sacrificed by decapitation, and their brains were dissected out, washed, and the hemispheres were cut into slices in frontal orientation using a vibratome (FTB, Plano, Marburg, Germany). Slice preparation was performed at 6°C in standard bath solution (see below). Subsequently, slices were stored for at least 30 min in the same solution at 35°C.

For the patch-clamp analysis in situ, slices (150 μm thick) were placed in a perfusing chamber installed on the stage of a Zeiss microscope (Axioskop FS, Zeiss, Oberkochen, Germany) and fixed in the chamber using a U-shaped platinum wire with a grid of nylon threads (Edwards et al., 1989). The chamber was continuously perfused with oxygenated standard solution and drugs were added to the bath as indicated. All recordings from glial cells were taken in the stratum radiatum of the hippocampal CA1 subregion (N = 118). The selected cells were located about 30 μm underneath the surface of the slice and could be approached by the patch electrode using water immersion optics. Positive pressure was applied to the recording pipette while it was lowered under microscopic control. Thus, cellular debris was blown aside and the tip could be placed onto the surface of a cell soma.

Solutions and Electrodes

The standard bath solution contained 124 mM NaCl, 5 mM KCl, 2 mM $CaCl_2$, 2 mM $MgCl_2$, 24 mM $NaHCO_3$, 1.25 mM NaH_2PO_4, and 10 mM glucose. In solutions containing high concentrations of $BaCl_2$ (10 mM) or tetraethylammonium (TEA, 16 mM), the NaCl concentration was reduced to ensure constant osmolarity. In all Ba^{2+} experiments, $H_2PO_4^-$ was omitted both in Ba^{2+}-containing as well as in the corresponding Ba^{2+}-free control solutions. By gassing the solutions with carbogen (5% CO_2/95% O_2), the pH was adjusted to 7.4. The pipette solution for in situ analysis contained 130 mM KCl, 0.5 mM $CaCl_2$, 2 mM $MgCl_2$, 5 mM ethylenebis(oxyethylennitrilo)tetraacetate (EGTA), 10 mM 4-(2-hydroxyethyl)-1-piperazineethanesulphonic acid (HEPES), 3 mM ATP, and 0.1% Lucifer Yellow (LY). Recording pipettes were fabricated from borosilicate capillaries (Hilgenberg, Malsfeld, Germany). LY (CH, dilithium salt) was from Fluka (Neu-Ulm, Germany). Unless otherwise stated, all other reagents were purchased from Sigma (Munich, Germany).

Recording Set-Up

Membrane currents were measured with the patch-clamp technique in the whole-cell recording configuration. Current signals were amplified (EPC-7 or EPC-9 amplifier, HEKA elektronik, Lambrecht, Germany), filtered at 3 or 14 kHz, and sampled at 6 or 80 kHz by an interface connected to an AT-compatible computer system, which also served as a stimulus generator. The resistance of the patch pipettes was 4–6 MΩ. The input resistance (R_i) was determined from currents elicited at the end of 10 mV voltage steps (duration 50 ms), which depolarized the membrane from −60 to −50 mV to minimize the activation of voltage-dependent conductances. Capacitance and series resistance (R_S) compensation (40–60%) were used to improve voltage clamp control. To assess the quality of voltage clamp control we applied the criteria established in our earlier work (Steinhäuser et al., 1990): 1) no "abdominable notches" or secondary humps in the current traces, 2) stable activation kinetics of voltage gated currents without any delay near threshold potential, and 3) graded current increase with small depolarizations beyond threshold potential. For the estimation of kinetic parameters, only recordings with residual voltage errors (resulting from the product $R_S I_{max}$) of less than 6 mV were evaluated. All voltages were corrected for liquid junction potentials.

To evaluate the viability of the slice preparation, we occasionally stimulated the Schaffer collaterals via a bipolar platinum electrode (resistance 40 MΩ, pulse amplitude 3–8 V, duration 50 μs) located in the stratum radiatum of the CA3 region and simultaneously recorded the postsynaptic responses in CA1 pyramidal neurons in the whole-cell mode. In these experiments, the distance between the platinum electrode and the recording electrode was at least 1 mm. Recordings were usually stable for up to 2 h and were accepted only if the initial resting potentials of the glial cells and neurons were negative to −65 mV and −50 mV, respectively.

Intracellular Staining of Cells and Immunocytochemistry

While recording in situ, cells were filled with LY by dialyzing the cytoplasm with the patch pipette solution. To reduce destruction of the cell by pulling off the pipette after recording, we destroyed the seal by a large hyperpolarizing current injection. For glial fibrillary acidic protein (GFAP)-staining, the slices were fixed in a solution containing 4% paraformaldehyde in phosphate buffered salt solution (PBS) for 2–5 days (pH 7.4, 5°C). The slices were washed in PBS (1 h) and incubated in ethanol at −20°C for 25 min. Subsequently, the tissue was washed in PBS several times. Swine serum (2%) and a GFAP antibody (1:200, Dako, Denmark) were added, and the slices were incubated in that solution for 12 h at 5°C. The slices were rinsed several times in PBS, swine serum was added, and the tissue was incubated in tetramethylrhodamine isothiocyanate (TRITC)-conjugated swine anti-rabbit immunoglobulins (1:100, Dako, Denmark) for 5 h at 5°C. After being washed in PBS and water, the slices were inspected in a Zeiss Axiophot light microscope equipped with fluorescence optics and fluorescein isothiocyanate (FITC) (BP 450–490, FT 510, LP 520) and TRITC (BP 546, FT 580, LP 590) filter combinations.

Immunolabelling for O antibodies was performed on cells acutely isolated from the CA1 stratum radiatum as described earlier (Steinhäuser et al., 1994b). After electrophysiological characterization, the patched cell was exposed to swine serum (10%), and after washing, the O1 or O4 antibodies (12.5 μg/ml, Böhringer, Mannheim, Germany) were applied for 20 min. The cell was rinsed, fixed in paraformaldehyde (4%, 10 min), and then Cy3-conjugated goat anti-mouse immunoglobulins (28 μg/ml, Dianova, Hamburg, Germany) were added for 20 min. The cell was washed and inspected under fluorescence optics. For control of unspecific labelling, the primary antibodies were omitted.

Data Analysis

The activation and inactivation parameters were calculated according to the Hodgkin-Huxley model (HH model) by means of a non-linear regression analysis based on the Gauss-Newton method (modified version of the program published by Schütz et al., 1984). The transient K^+ currents were fitted to the equation $I(t) = I_0[1 - a \exp(-t/\tau_n)]^4[b + \exp(-t/\tau_g)]$ with I_0 being the current amplitude as inactivation remained at rest, τ_n and τ_g being the time constants for activation and inactivation, and a and b were amplitude factors.

All data are given as mean ± SD. Significant differences between data were evaluated by the use of the Student's t-test. The level of significance was set at $P \leq 0.05$.

RESULTS

Cell Identification

By combining ultrastructural inspection with immunocytochemical and electrophysiological characterization, various types of glial cells can be distinguished in the postnatal mouse hippocampal slice (Steinhäuser et al., 1992, 1994a). Even though these studies were performed with animals at the same developmental stage (p9–12), the cells displayed intriguing differences with respect to their ion channel phenotypes.

In the present study, we focused on glial cells expressing the characteristic "complex" pattern of different K^+ and Na^+ currents (Steinhäuser et al., 1994b). These cells were small in diameter (about 5–8 μm), and various thin processes extended from the cell body (Figs. 1a, 2e). Despite prominent changes in their electrophysiological properties, we could not observe marked changes in the morphological appearance of the cells with increasing age. In bright field microscopy, cell bodies displayed a lucent halo and dark cell boundaries and thus could be clearly distinguished from another glial cell type in the same hippocampal subregion, which was characterized by the sole expression of voltage- and time-independent K^+ channels ("passive" cells). The few neurons in the stratum radiatum were much larger (Fig. 1d, 15–20 μm; cf. Minkwitz, 1976), and their resting potentials were positive (−53.8 ± 3.9 mV, N = 11, p9–12) to those recorded in the glial cells (see below and Steinhäuser et al., 1994b). By depolarizing the neurons, Na^+ currents were activated in the voltage clamp mode which were at least one order of magnitude larger as compared to I_{Na} in the "complex" cells (Fig. 1e). In all neurons analyzed, positive current injections generated action potentials thereby depolarizing the membrane to 16.2 ± 4.8 mV (N = 5, Fig. 1f). Some of the stratum radiatum neurons displayed spontaneous firing at resting potential (Fig. 1f), similar to what was observed in other nonpyramidal hippocampal neurons (Schwartzkroin and Mathers, 1978; Williams et al., 1994). In contrast, however, glial cells not only lacked any spontaneous activity, but, the glial Na^+ currents were never observed to generate action potentials by applying depolarizing currents up to 90 pA in the current clamp mode (N = 29) which depolarized the cells by up to 65 mV (Fig. 1c). This lacking spike activity is most probably due to the low Na^+ to K^+ conductance ratio ob-

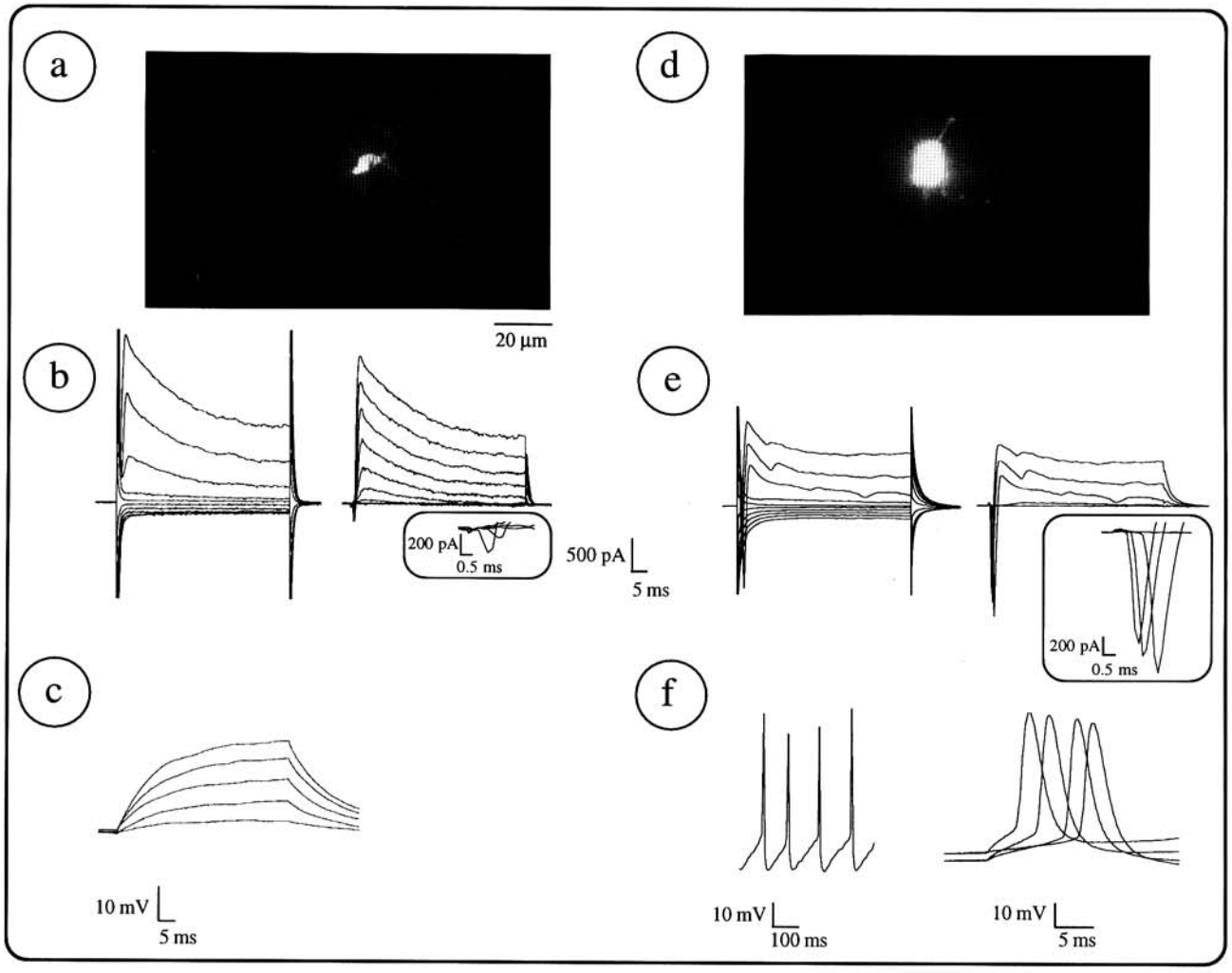

Fig. 1. Properties of "complex" glial cells (a–c) and neurons (d–f) in hippocampal brain slices. A p5 "complex" cell was recorded in the CA1 stratum radiatum and thereby was filled with LY by dialyzing the cytoplasm with the patch pipette solution (a). For current activation, the membrane was stepped to increasing de- and hyperpolarizing potentials ranging between −160 and 20 mV (duration 50 ms, 20 mV increment, holding potential −70 mV) (b, left). Subtraction of capacitance artefacts and passive currents revealed a small net inward current when the cell was depolarized beyond −40 mV (b, right). The inset demonstrates the current responses obtained at 20, 0, −20, −40, and −60 mV with a higher resolution. A maximum inward current of 245 pA was registered at 10 mV. (c) Depolarizing current injections of up to 90 pA (20 pA increment) did not activate action potentials in the glial cells. A neighbouring stratum radiatum neuron was analyzed as described above. The soma was much larger (d), and depolarizing voltage steps activated transient inward currents of up to 1470 pA (inset in e). The neuron displayed spontaneous firing at resting potential (−52 mV), depolarizing the cell to about 17 mV (f, left). Action potentials were generated in the current clamp mode (current injections of 10 to 70 pA, 20 pA increments) with the delay decreasing when the command curents increased (f, right).

served in acutely dissociated "complex" glial cells (0.21, Steinhäuser et al., 1994b) or in situ (0.08, Sontheimer and Waxman, 1993).

During the recordings, the cells were dialyzed with the pipette solution and thereby filled with LY. Subsequently, the slices were stained for glial fibrillary acidic protein (GFAP), a marker that recognizes mature astrocytes (Eng. 1985). At p9, we never observed a positive GFAP staining of the "complex" cells (N = 15). In contrast, 3 out of 12 cells at p30 were weakly GFAP-positive (Fig. 2d–f). These findings confirm our earlier observations in situ (Steinhäuser et al., 1994a) and agree with data obtained from cells acutely isolated from the same brain subregion (Steinhäuser et al., 1994b; Tse et al., 1992) that also hinted at an upregulation of GFAP in "complex" glial cells between p5 and p35. In addition, northern blot analysis and in situ hybridization studies have shown that GFAP mRNA in the hippocampus accumulates during postnatal development, with the greatest increase occurring after p10 in the rat (Landry et al., 1990). It is very unlikely that the lack of staining in GFAP-negative cells in our study was due to bad penetration of the antibodies because we found GFAP-positive cells in the close vicinity to the GFAP-negative cells which the recordings were taken from. Furthermore, "complex" cells acutely isolated from the CA1 stratum radiatum between p5 and p12 could not be labelled with the surface antibodies O1 (N = 5) or O4 (N = 4) which

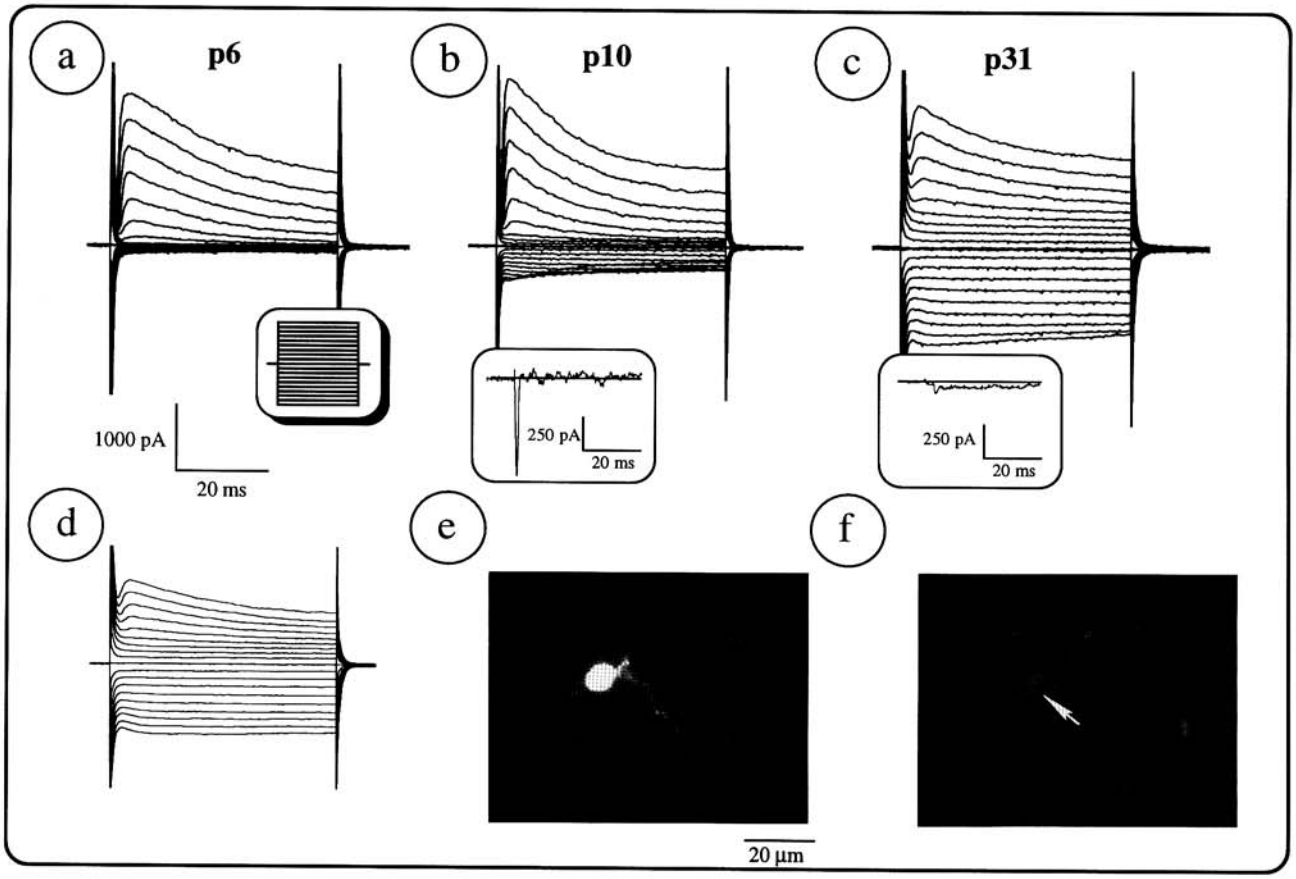

Fig. 2. Changes in membrane current pattern of "complex" glial cells during development. For current activation, the membrane was stepped to increasing de- and hyperpolarizing potentials between −160 and 20 mV (duration 50 ms, 10 mV increment, holding potential −70 mV, see the shaded inset for voltage commands). a, b: At p6 and p10, large outwardly rectifying K^+ currents were activated if the membrane was depolarized beyond −30 mV. These currents were mainly composed of a transient and a sustained component. Occasionally, a small, inactivating inward rectifier current was observed in the p9 group. A prominent sodium inward current could be isolated in the p10 cell by subtracting membrane currents recorded in 1 µM TTX containing bath solution from the control currents. The inset in b shows I_{Na} at a membrane potential of 0 mV. The resting potentials were −73 mV in both cells. c: At a later stage of development, all cells expressed inward rectifier channels. In addition, a prominent time- and voltage-independent current appeared, while the outwardly rectifying components were down regulated. Only tiny Na^+ currents could be detected in this cell applying the procedure described above. The resting potential was −78 mV. A p30 "complex" cell was recorded in the CA1 stratum radiatum (d) and thereby was stained with LY (e). Subsequently, the slice was immunolabelled with an antibody against GFAP. Immunolabelling with a TRITC-conjugated second antibody (f) shows a positive staining of the LY stained cell.

TABLE 1. Passive membrane properties of "complex" glial cells during ontogenesis

Age	p5	p9	p20	p30
Resting potential [mV]	−71.0 ± 2.6	−71.5 ± 4.0	−73.9 ± 3.8	−74.7 ± 2.5
Input resistance [GΩ]	0.5 ± 0.2	0.4 ± 0.3	0.1 ± 0.1	0.1 ± 0.03
Cell number	14	20	11	27

identify glial precursor cells and oligodendrocytes (Sommer and Schachner, 1981). Our results thus strongly suggest that the "complex" glial cells represent a subpopulation of immature astrocytes.

Passive Membrane Properties

We compared the relative contribution of the various Na^+ and K^+ currents to the whole membrane current pattern as well as the passive membrane properties of "complex" cells during different stages of the postnatal development. All recordings were obtained from cells located in the hippocampal CA1 stratum radiatum subregion, and the cells were grouped as follows: p5 (p5–6), p9 (p9–12), p20 (p20–25), and p30 (p30–35). Table 1 compares the resting potential and input resistance (R_i) registered in the corresponding periods. Between p5 and p30 both parameters significantly changed, indicating an increasing resting K^+ conductance with cell maturation. In cells of the p30 group, the resting potential closely matched the K^+ equilibrium potential of $E_K = -77$ mV (assuming an activity coefficient $\gamma = 0.79$,

T = 22°C). The decrease in R_i during development is comparable to corresponding data obtained in CA1 pyramidal neurons (Spigelman et al., 1992). In contrast, the neuronal resting potentials observed in the latter study were much more positive as compared to those of the glial cells (taking into account the different E_K values due to the variable ionic gradients imposed) but they also shifted to more negative values with age.

Sodium Currents

The Na^+ current density of dissociated "complex" cells at p9–12 (4.2–24.2 pA/pF, Steinhäuser et al., 1994b), in situ (1.5–90 pA/pF, Sontheimer and Waxman, 1993), and in cultured hippocampal astrocytes (4.2–34.6 pA/pF, Sontheimer et al., 1991a) was found to be much less than in cultured (219.5 pA/pF, Sontheimer et al., 1991a) or acutely isolated hippocampal neurons (3–30 nA/5–50 pF which gives about 500–600 pA/pF, cf. Steinhäuser et al., 1990; Sah et al., 1988). Since the patch-clamp recordings in slices suffer from limited voltage clamp control, the kinetic and stationary properties of fast sodium inward currents were recently analyzed in dissociated hippocampal glial cells (Steinhäuser et al., 1994b). Consequently, in the present in situ study we could only qualitatively estimate the expression of I_{Na} during ontogenesis. To remove inactivation of the glial I_{Na}, the depolarizing test pulses were preceded by conditioning hyperpolarizing prepulses to −110 mV (duration 300 ms). Under these conditions, inactivation was shown to be negligible with I_{Na} reaching more than 90% of the maximum values (Steinhäuser et al., 1994b). For the isolation of I_{Na}, membrane currents were evoked in control solutions and the cells were subsequently exposed to solutions containing 1 μM TTX which completely blocked the glial Na^+ currents. Subtracting the recordings obtained at corresponding membrane potentials in control solution and in TTX solution, in all p5 (N = 11) and 86% of the p9 cells (N = 21) voltage dependent sodium inward currents of up to 650 pA were detected (Fig. 2b, inset). During the next three weeks, the percentage of cells possessing I_{Na} significantly decreased (Fig. 2c, inset). In the p30 group, we could detect Na^+ inward currents only in 1 out of 16 cells by applying the TTX subtraction protocol (maximal amplitude 150 pA). The disappearance of I_{Na} was not due to deteriorated clamp conditions caused by the decreasing membrane resistance because even in Ba^{2+} containing solution, i.e., under conditions which largely increased the membrane resistance and reduced fast outward currents, no or only tiny Na^+ currents were observed in the older cells (cf. Fig. 8b).

Potassium Currents

In the immature hippocampus (p5–12), the current pattern of "complex" glial cells was dominated by voltage activated transient (I_A) and delayed rectifier outward K^+ currents (I_K). During the next two weeks of postnatal maturation, we observed a progressive increase in inward rectifier currents (I_{IR}) evoked by hyperpolarizing commands which in most cases displayed inactivation at voltages negative to −130 mV. In addition, a time- and voltage-independent passive component appeared after p12 (Fig. 2).

The following experiments were aimed at a quantitative evaluation of the regulation of these four current components during ontogenesis. It was difficult to estimate the cell surface area of the "complex" cells in situ, and in particular, we could not exclude changes of this parameter with time. Therefore, to get a quantitative measure of the contribution of the different currents to the whole current pattern, we calculated the ratios of the corresponding membrane conductances at the different stages of maturation. Most of the recordings were taken in TTX-containing solutions to block voltage gated Na^+ channels. A noticeable contribution of inward currents through voltage gated Ca^{2+} channels could be excluded in the "complex" glial cells because it was shown that these currents are very small (maximum amplitudes less than 150 pA) and disappear almost completely within a few minutes after breaking the seal in the conventional whole cell mode (Akopijan and Steinhäuser, unpublished observation). Accordingly, even under conditions that reduce K^+ outward currents and facilitate currents through voltage gated Ca^{2+} channels (superfusion of 10 mM Ba^{2+}), no inward currents could be detected, stepping the membrane potential up to 20 mV (see Fig. 8b).

Sustained outward currents

Sustained outward currents were isolated when the transient component was inactivated by applying depolarizing prepulses prior to current activation. In the young cells (p5–12; Fig. 3a–c) the sustained component mainly consisted of the TEA-sensitive, Ca^{2+}-independent delayed rectifier current, as described previously (Steinhäuser et al., 1994b). In contrast, in p20 and p30 cells an additional, voltage-independent current appeared which could not be blocked by bath application of either TEA (16 mM, N = 21) or 4-AP (4 mM, N = 21) and clearly dominated the I/V relation in the older cells (Fig. 3d–f).

To determine the ionic selectivity of the passive currents, the reversal potential (V_{rev}) was determined for each individual cell by a linear regression of the currents evoked in the subthreshold potential range (between −40 and −60 mV, see inset in Fig. 4c). V_{rev} varied between −71.7 ± 19.0 mV (p5, N = 11) and −82.8 ± 7.4 mV (p30, N = 16), indicating that these currents were also largely carried by K^+ and were only little contaminated by unspecific leak currents. The passive membrane conductance, g_p, was calculated by dividing the subthreshold currents by their corresponding driving force, $V - V_{rev}$. Subsequently, the passive currents were determined from g_p for the whole voltage range

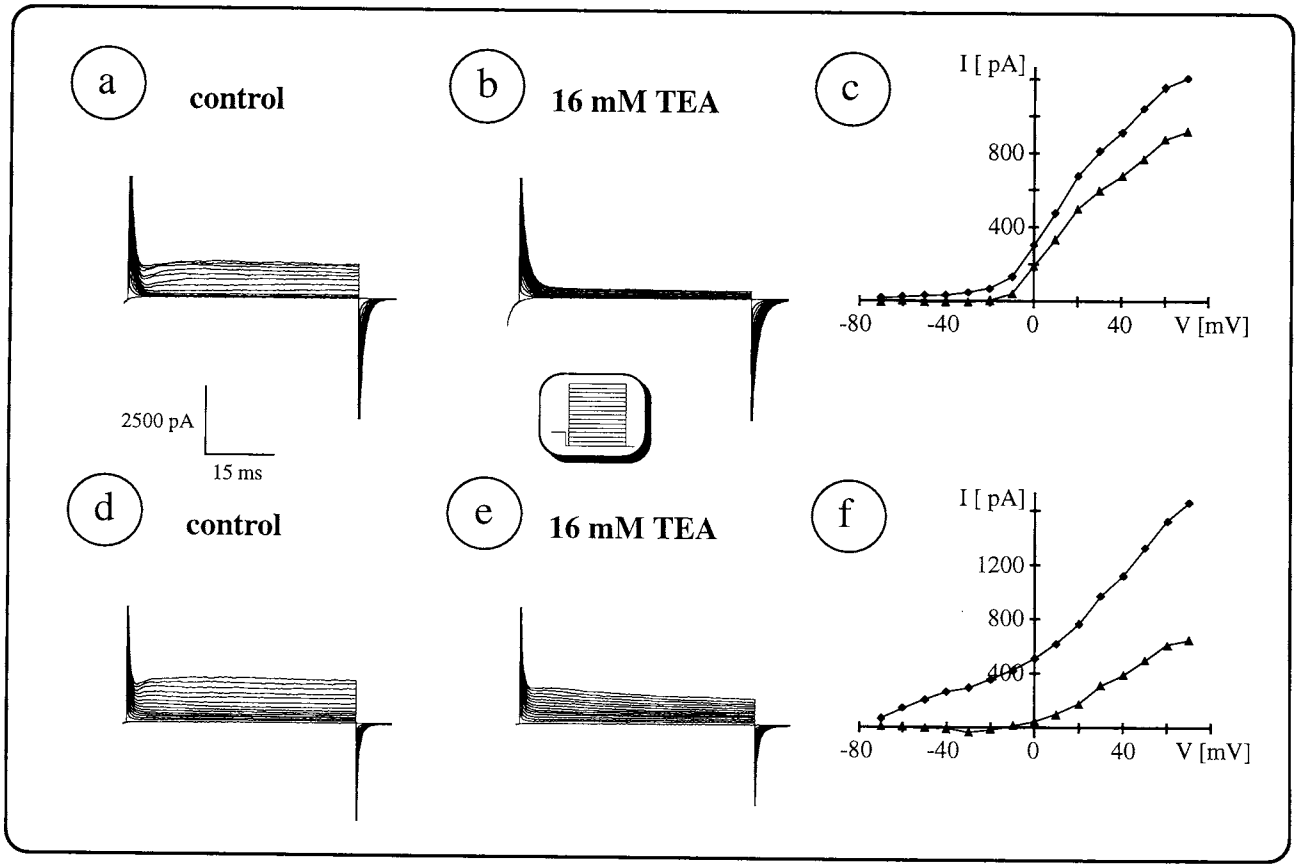

Fig. 3. TEA sensitivity of sustained outward K^+ currents. Recordings were obtained from a p10 "complex" cell (a–c) and at p30 (d–f). a, d: The sustained outward currents were isolated from the whole outward current if the membrane was depolarized to −40 mV prior to current activation. This prepulse (300 ms) was followed by a 3 ms interval at holding potential (−70 mV), and then the membrane was stepped to increasing depolarizing potentials (50 ms, 10 mV increment) up to 70 mV (see the shaded inset for voltage commands). The resting potentials were −79 and −75 mV, respectively. b, e: Addition of 16 mM TEA largely reduced the outward current in the p10 cell (block to 24%) while the effect in the older cell was much less (block to 57%). In both cells the block was partly reversible. After wash out, the currents reached 62% (p10) and 84% (p30) of the amplitudes observed before drug application (not shown). c, f: The TEA sensitive component (triangles) was obtained by subtracting the currents measured in 16 mM TEA from the corresponding control currents. Comparing the I/V-curves of the control currents (squares) and the TEA sensitive component demonstrated that the passive conductance was not affected by TEA. Note the increase in the slope factor of the I/V curve for the sustained currents in the older cell between −70 and −40 mV, hinting at an up-regulation of the passive conductance with maturation. No significant change in the threshold potential of the TEA sensitive component was observed during ontogenesis. All recordings were taken in TTX-containing bath solution.

(−70–70 mV) and were subtracted from the sustained currents at corresponding membrane potentials. Thus, I_K was isolated (Fig. 4a,b) and g_K was calculated by dividing I_K at different membrane potentials by the actual driving force, $V - E_K$. It is possible that we slightly overestimated the passive conductance because in some cells, inward rectifier channels were already active between −40 and −60 mV (see below). Comparing the ratios of the conductances, g_K/g_P (V = 70 mV), an opposite regulation of both components became obvious between p5 and p30 (Fig. 4c). During the first 2 weeks of postnatal development, g_K exceeded g_P by far while in the p30 cells, it reached just about 25% of the passive conductance with the differences being statistically significant. I_K showed a substantial reduction superfusing the cells with TEA. In contrast, the delayed rectifier was much less sensitive to application of 4-AP (cf. Table 2). We could not reliably quantify the properties of I_K in the more aged cells due to the considerable down-regulation of that component after p9.

We have previously reported on the rare appearance of dye coupling in glial cells of the 9–12-day-old hippocampus in situ (Steinhäuser et al., 1994a). In the present study, a spread of LY to adjacent cells was observed in 3 out of 26 "complex" cells at p30. It is known that weak electrical coupling between glial cells does not necessarily imply the presence of dye coupling (Ransom and Kettenmann, 1990). To test whether the increase in passive currents in the older cells was due to an enlarged contribution of voltage-independent junctional currents (Kettenmann and Ransom, 1988), coupling was blocked with halothane (10 mM; Dermitzel et al., 1991). We compared the passive conductance (calculated as described above) and the membrane transients prior to and in the presence of halothane. Halothane affected the current responses in 4 out of 7 "complex" cells tested

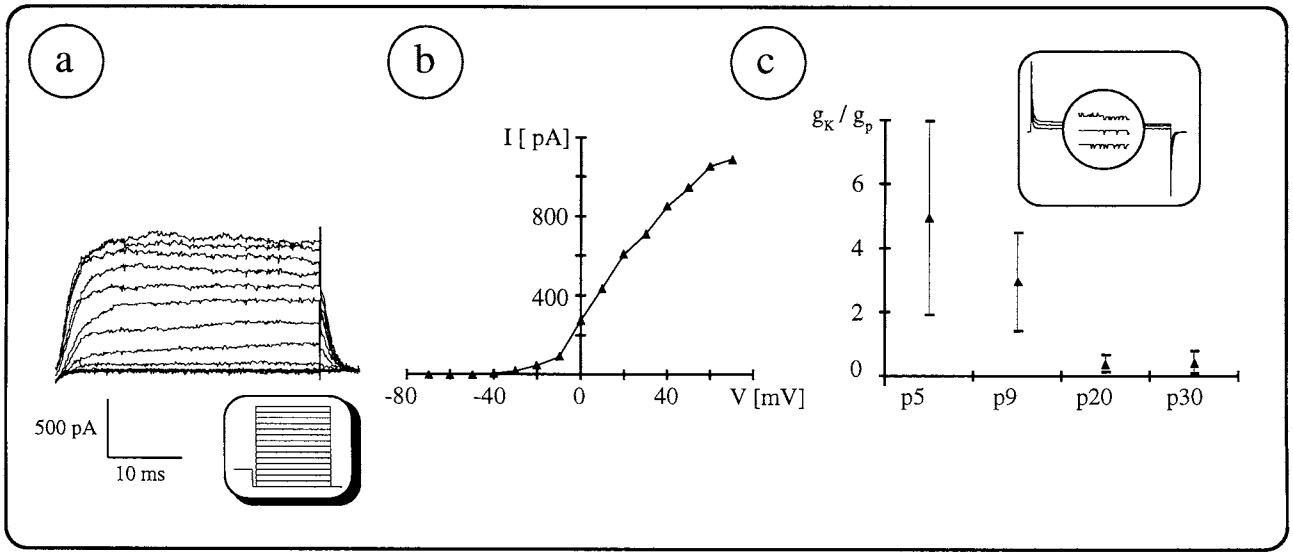

Fig. 4. Developmental regulation of delayed rectifier K^+ currents. a: Sustained outward currents were isolated from the whole outward currents as described in the legend to Figure 3a. Subsequently, I_K was separated by subtracting capacitance artefacts and passive currents from the sustained currents at corresponding membrane potentials. Currents were taken from a cell at p10, the resting potential was −79 mV; 1 μM TTX was added to the bath solution to block voltage gated Na^+ channels. b: The I/V curve of I_K revealed a threshold for current activation at −20 mV. c: The sustained outward currents activated at 70 mV were subtracted by the corresponding passive current component which was calculated from g_P. After that, the conductance g_K was determined at 70 mV by dividing the remaining amplitudes by the actual driving force, $V - E_K$. The passive conductance, g_P, was calculated from the time-independent currents activated in the subthreshold range (−60 to −40 mV, see inset in c). Finally, the ratio g_K/g_P was compared during maturation, revealing a significant decrease between p5 and p20. Values were determined from at least 8 and at most 22 cells.

TABLE 2. Pharmacological properties of glial K^+ currents during development[a]

	16 mM TEA						4 mM 4-AP					
	A-current, I_A			Delayed rectifier, I_K			A-current, I_A			Delayed rectifier, I_K		
Age	Mean	SD	N	Mean	SD	N	Mean	SD	N	Mean	SD	N
p5	0.85	0.10	6	0.28	0.04	5	0.54	0.25	5	0.62	0.31	4
p9	0.76	0.11	5	0.18	0.04	5	0.23	0.06	9	0.67	0.18	9
p20	0.85	0.22	10	n.d.	n.d.	n.d.	0.33	0.09	3	n.d.	n.d.	n.d.
p30	0.90	0.15	4	n.d.	n.d.	n.d.	0.33	0.09	5	n.d.	n.d.	n.d.

[a]Values represent the portion of currents insensitive to the corresponding substances. Data were taken at V = 70 mV. n.d., not determined.

at p30 with the passive conductance decreasing to 74 ± 10% (Fig. 5a,b). One of the few cells which exhibited both noticeable characteristics of electrical as well as dye coupling is shown in Figure 5.

Transient outward K^+ currents

"Complex" cells possessed prominent transient outward currents (I_A) at all ages analyzed. This current was separated as previously described (Steinhäuser et al., 1994b). To remove current inactivation, the membrane was hyperpolarized to −110 mV for 300 ms prior to the recordings. Subsequently, I_A was isolated from the total outward currents by subtracting the current family obtained after a prepulse to −40 mV at corresponding voltages (cf. insets in Fig. 6a,b). In our earlier work, we could demonstrate a voltage dependence of the 4-AP block of I_A in the "complex" cells at p9 (Steinhäuser et al., 1994b). Here we show that the 4-AP sensitivity of the transient current significantly changed during ontogenesis. In the p5 cells, the block by 4 mM 4-AP was less than half as effective as compared to the p9 cells (Table 2). To compare the kinetic properties of I_A, the time constants of current activation (τ_n) and inactivation (τ_g) were calculated according to the Hodgkin-Huxley model. There was a significant increase both in τ_n and τ_g between p10 and p20, while no consistent changes could be detected between the p5–p10 and the p20–p30 groups (Fig. 6d,e).

We calculated the membrane conductance, g_A, dividing the peak currents evoked between −70 and 70 mV by their driving force, $V - V_K$. Comparing the relative contribution of g_A and g_P, a significant decrease in the transient component was observed with continued development (Fig. 6f). At the same time, the drop of g_K was more pronounced than the down-regulation of g_A (Fig. 6g).

Inward rectifier K^+ currents

In addition to the appearance of passive currents, all older cells (p20–35) possessed prominent inward recti-

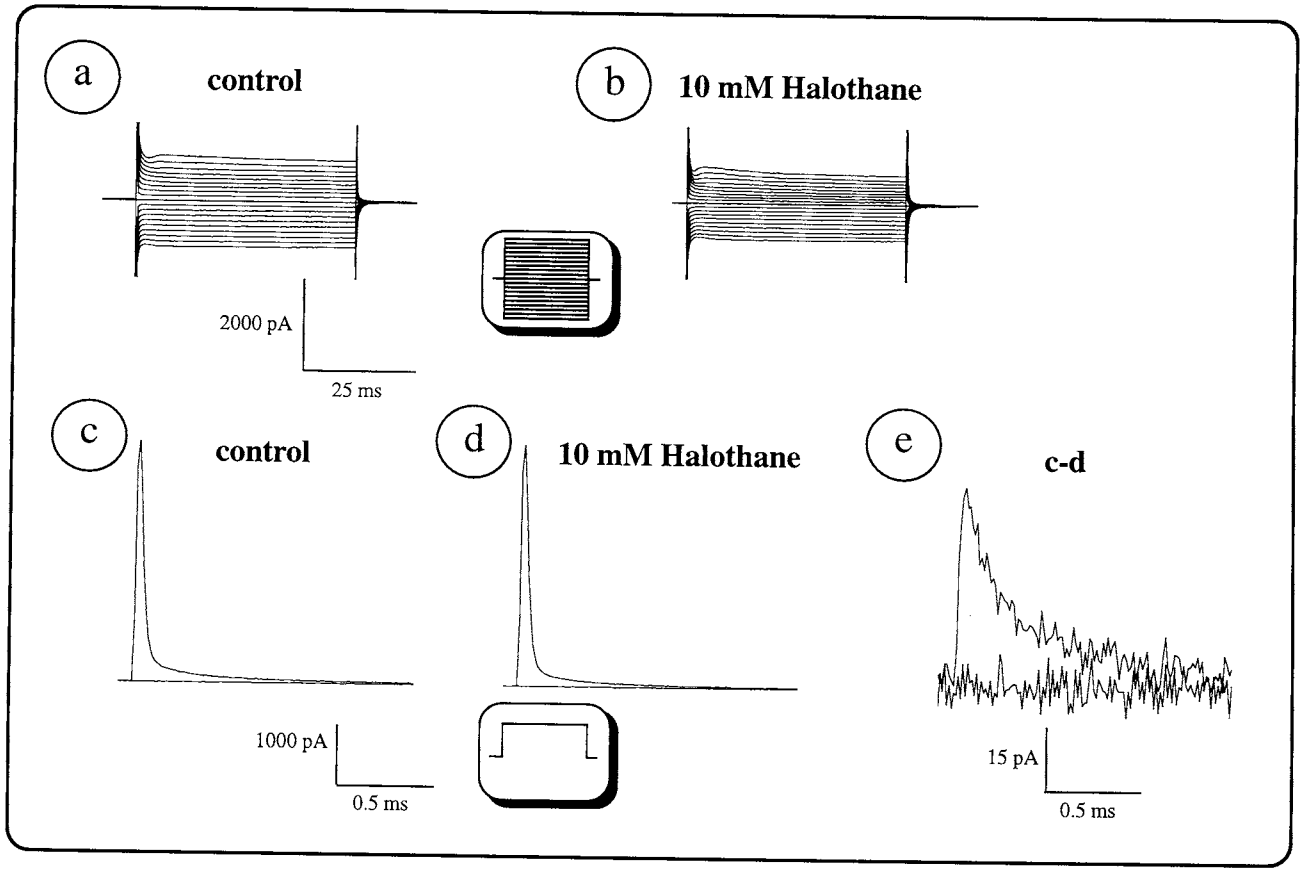

Fig. 5. Electrical coupling between glial cells. **a, b:** Membrane currents were activated in a p30 cell as described in the legend to Figure 2 (for voltage commands see the shaded inset). In this case, LY was observed to spread to adjacent cells. During exposure to halothane (10 mM, saturated concentration), a decrease in the passive conductance from 9.8 to 5.8 nS was observed, which partly recovered during rinsing. The resting potential was −79 mV in normal bath solution. **c–e:** Changes in the cell capacitance were measured by comparing the current transients in the same cell in normal bath solution and after uncoupling the cells with halothane. After compensation for passive currents, five depolarizing voltage steps to −60 mV were applied. The current responses were recorded with high resolution (filter 14 kHz, sampling rate 80 kHz) and averaged. Subtracting both traces (e), a difference remained with the integral of this halothane-sensitive current being a measure for the change in the charge transferred across the membrane.

fier currents (I_{IR}) applying hyperpolarizing voltage jumps (Fig. 7). In most cells, the currents showed a voltage-dependent inactivation negative to −130 mV, and the decay could be well described by a monoexponential function with the time constant of inactivation decreasing as the membrane potential became more negative (not shown, see Steinhäuser et al., 1992). Such currents were only rarely detected in p5 and p9 cells. To test for the K^+ sensitivity of the inward currents, the reversal potential was determined in bath solutions containing 5 and 50 mM $[K^+]_o$. Voltage ramps were applied which continuously changed the membrane potential between −140 and 90 mV within 1 s. To reduce the contribution of g_A and g_K, the recordings were taken in solutions containing 16 mM TEA and 4 mM 4-AP. Since the passive conductance was not sensitive to these substances, we selected cells from the p9 group which lacked a prominent g_P but already expressed significant inward rectifier currents (Figs. 2b, 7a). Two important changes were observed as $[K^+]_o$ was increased. First, the zero-current potential shifted by 51.1 ± 2.9 mV (range 48.7 to 54.9 mV, N = 4) toward positive membrane potential in the high $[K^+]_o$ solutions (Fig. 7c). This shift was very close to that predicted by the Nernst equation for a K^+ selective membrane (ΔV = 53 mV, assuming γ = 0.85 and 0.79 for 50 and 130 mM K^+, respectively), indicating that the channels were predominantly permeable to K^+ ions. Second, the conductance was significantly increased in high K^+ solutions which is also typical of inward rectifying K^+ channels and can be described by the Goldman-Hodgkin-Katz equation (Sakmann and Trube, 1984). Extracellular Ba^{2+} (10 mM) inhibited I_{IR} to less than 4% of the control currents (V = −120 mV) both in p9 cells (N = 10) and at p20 (N = 6) (Fig. 8a–c).

To correlate the expression of inward rectifier channels with the developmental state, the relative contribution of the conductance, g_{IR}, was compared to the whole voltage-gated outward conductance, g_{out}, in each individual "complex" cell between p5 and p30. The traces were compensated for the passive currents, and the data were calculated from the remaining peak currents evoked in response to voltage jumps to 20 and −130 mV, respectively (holding potential −70 mV). Figure 8d illustrates that the inward rectifier K^+ currents domi-

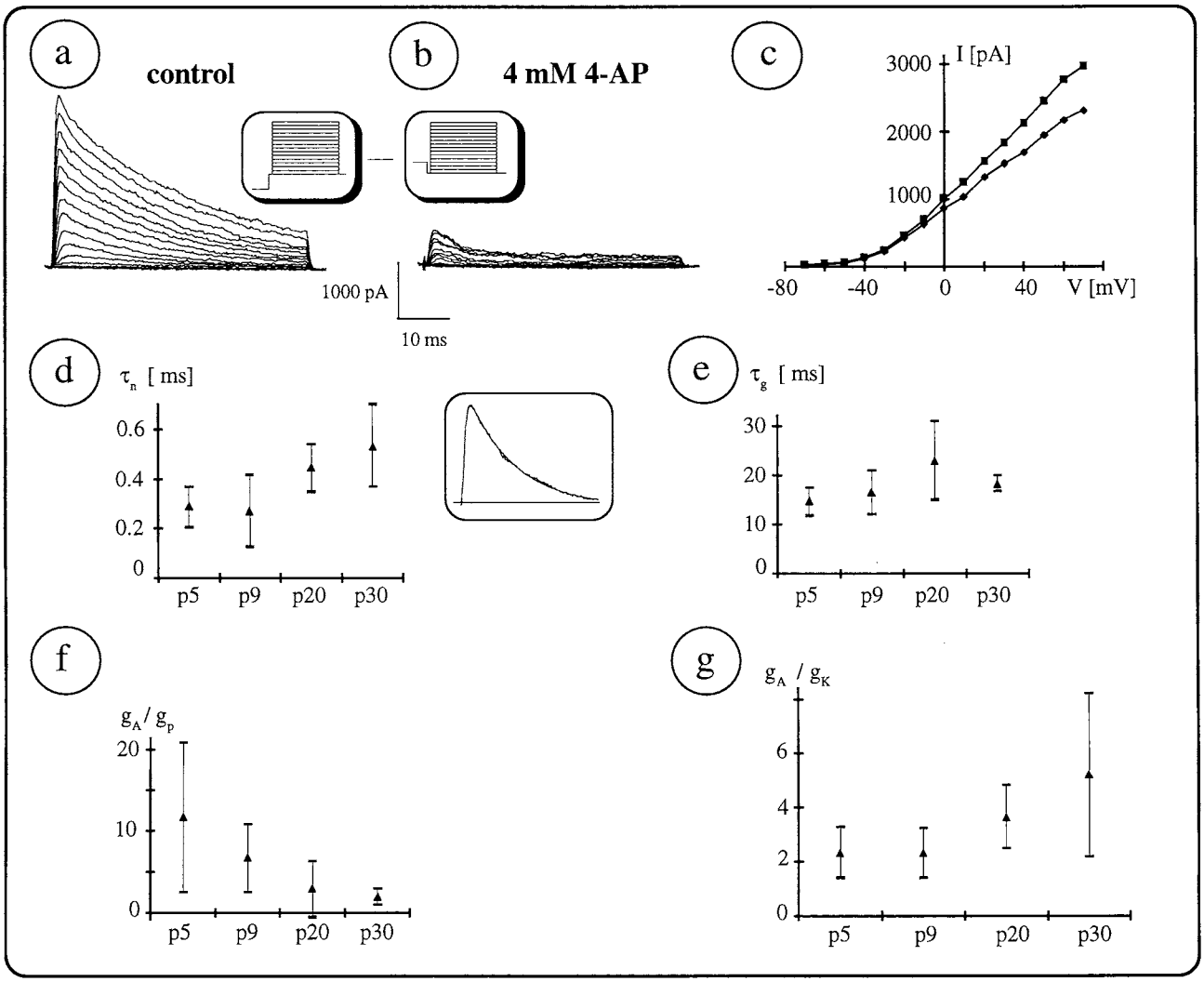

Fig. 6. Developmental regulation of glial A-type currents. a: To remove inactivation of I_A, the membrane was hyperpolarized to −110 mV prior to the recording (prepulse duration 300 ms). After a 3 ms delay at holding potential (−70 mV), outward currents were evoked by applying depolarizing voltage steps between −70 mV and 70 mV (50 ms, 10 mV increment). To separate I_A from the whole outward current, the sustained component (see Fig. 3) was subtracted from the current family induced after the −110 mV prepulse at corresponding membrane potentials (for pulse protocol see shaded insets). The recordings were taken from a p10 cell in TTX-containing external solution. b: Bath application of 4-AP reversibly reduced the transient currents. Before drug application, the resting potential was −74 mV. c: Both the I/V curve of the whole transient current (squares) and that of the 4-AP-sensitive currents (diamonds) revealed threshold potentials of about −40 mV. d, e: Current responses were recorded at 70 mV and were fitted according to the n^4g model (see Materials and Methods). The inset demonstrates a current trace together with the superimposed fitted data (smooth line). Subsequently, the corresponding time constants of activation (τ_n) and inactivation (τ_g) were compared during development, revealing a significant increase in both time constants at p20. The cell number in the different age groups varied between 6 and 10. f: The relative contribution of transient and passive currents were compared during ontogenesis. Although g_A (determined at 70 mV) dominated in p5 and p9 cells, a significant decrease in the ratio was observed after p5, despite the considerable variability of the data in the immature cells. The number of cells analyzed at the different stages was between 9 and 23. g: g_A and g_K were calculated at 70 mV in TTX containing solution as described above and were compared during ontogenesis. A significant increase in the ratio was observed after p9. The cell number varied between 8 and 22.

nated in the more mature cells, but in the young cells they were only occasionally met.

DISCUSSION

In the present study, we evaluated changes in the relative contribution of a Na^+ and four different K^+ conductances (g_A, g_K, g_P, and g_{IR}) to the current pattern of a subpopulation of glial cells, termed "complex" cells, during maturation between p5 and p35 in situ. To limit the variability due to the regional glial heterogeneity (cf. Patel, 1986; Wilkin et al., 1990), all recordings were taken from cells located in the CA1 stratum radiatum region. These investigations thus extend our earlier report that provided a quantitative analysis of the kinetic and pharmacological properties of g_{Na}, g_A, and g_K at p9–12 (Steinhäuser et al., 1994b). Besides their electrophysiological characteristics, the identification of the "complex" cells is based on morphological and immunocytochemical data. Since these cells did not express O1

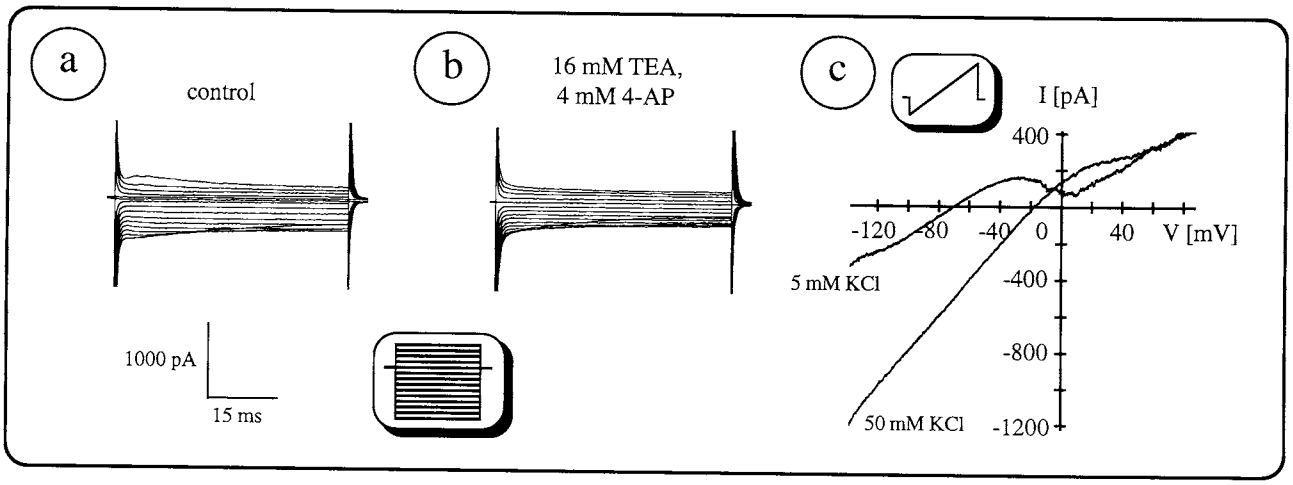

Fig. 7. Glial inward rectifier currents are mainly carried by K^+. a: Starting from a holding potential of −70 mV, outward and inward currents were activated in a p10 cell by stepping the membrane between −160 and −20 mV (duration 50 ms, 10 mV increment, see inset). b: To separate inward rectifier currents, the voltage-dependent outward K^+ currents were blocked by adding TEA (16 mM) and 4-AP (4 mM) to the bath solution. c: Voltage ramps were applied to the same cell in normal or elevated K^+ concentrations which continuously changed the membrane potential between −140 and 90 mV within 1 s (see inset). TEA and 4-AP were added to both solutions to block A-type and delayed rectifier outward currents. Changing the K^+ concentration in the bath solution from 5 mM to 50 mM shifted the zero-current potential by 51.6 mV, indicating that the currents were predominantly carried by K^+. The resting potential was −75 mV before drug application.

and O4 antigens while some of them were positively stained for GFAP at the later developmental stage, we assume that these cells represent a population of immature astrocytes. This was substantiated by very recent immunocytochemical investigations using a new monoclonal antibody which binds to a surface antigen of cells that differentiate to astroglial cells (Seifert et al., 1995). The assumption is also in line with a study of the Heinemann group that followed the development of astrocytes in the rat hippocampus, demonstrating a sevenfold increase in the number of GFAP-positive cells between p8 and p24 in the CA1 stratum radiatum (Nixdorf-Bergweiler et al., 1994).

Na^+ Currents During Cell Development

The functional significance of glial Na^+ currents is still unknown, but it has been suggested that glial cells may synthesize Na^+ channels that are incorporated into axonal membranes (Ritchie, 1992). Alternatively, these currents were thought to be involved in the regulation of the glial Na^+/K^+-ATPase (Gautron et al., 1992; Sontheimer, 1994). Recently, an electrogenic Na^+/HCO_3^- cotransport was described in mouse and rat cortical astrocytes (Brookes and Turner, 1994; O'Conner et al., 1994) which could be influenced by changes in $[Na^+]_i$ mediated by voltage-gated Na^+ currents. In the present study, Na^+ current-possessing "complex" glial cells were mainly found in slices prepared from mice before p12 but were almost absent at p30. This observation agrees with data of Sontheimer et al. (1991a) obtained in rat hippocampal astrocytes in which a significant loss in cells expressing I_{Na} after 10 days in culture was found. In contrast to Sontheimer and Waxman (1993), we did not observe Na^+ currents in GFAP-positive cells. However, these cells were located in the stratum oriens and close to the granule cell layer. It is possible that the expression pattern of astrocyte properties differs in the hippocampal subregions; the density of GFAP-positive cells in these laminae is higher and reaches the adult values earlier than in the stratum radiatum (Nixdorf-Bergweiler et al., 1994). It seems obvious that the lack of I_{Na} in acutely isolated hippocampal astrocytes at p25–35 reported by Tse et al. (1992) also most probably reflects Na^+ channel downregulation rather than a localisation of the channels on distal processes that were sheared off by the dissociation procedure. In addition, Na^+ currents were preserved in these cells isolated earlier in development (Steinhäuser et al., 1994b). This decrease in I_{Na} goes hand in hand with a time-dependent increase of cells coupled via gap junctions. However, we also found many cells between p20 and p35 with negligible Na^+ currents which still did not possess any signs of electrical or dye coupling. These observations in situ resembled findings in cell culture (Sontheimer et al., 1991b). Thus, the development of glia Na^+ channels is quite opposite to that observed in neurons of various brain areas. Both patch clamp studies on acutely dissociated cortical neurons (Cummins et al., 1994) as well as saxitoxin-binding experiments on hippocampal neurons in situ (Dargent et al., 1994; Xia and Haddad, 1994) demonstrated that Na^+ channel density increase with postnatal age, reaching a maximum level only after p12, i.e. at a stage when glial Na^+ currents are already down regulated. There is no doubt that astrocyte Na^+ channel expression is modulated by neurons (Barres et al., 1990; Minturn et al., 1992). In cultured spinal cord astrocytes, a down regulation of the glial Na^+ currents was observed in neuron-conditioned

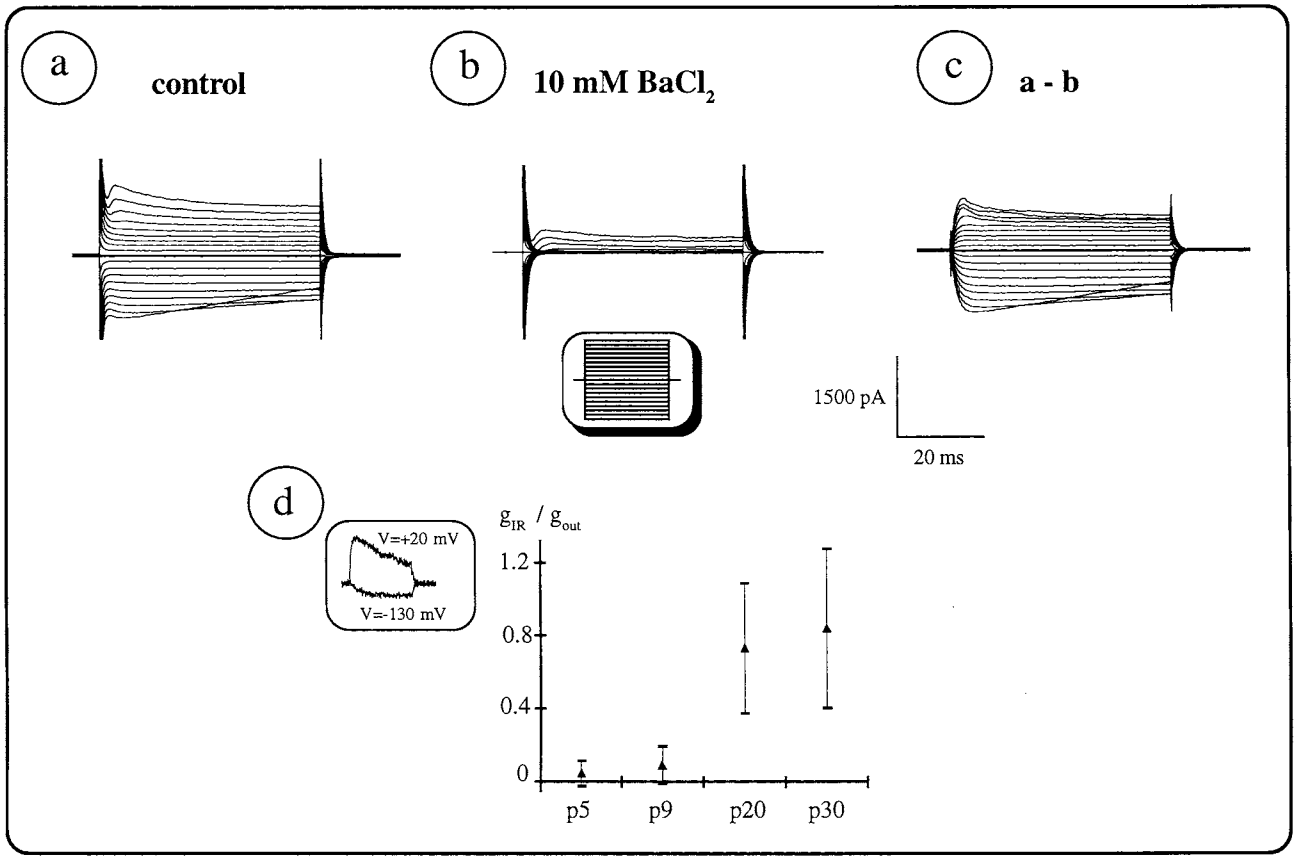

Fig. 8. Inwardly rectifying K^+ currents are up-regulated during ontogenesis. **a, b:** Membrane currents were obtained from a p22 "complex" cell (resting potential −76 mV) by stepping the membrane between −160 and 20 mV (cf, legend to Fig. 2 and shaded inset). Inactivation of inward rectification was observed at potentials negative to −130 mV. The inwardly rectifying K^+ channels were completely blocked by adding 10 mM Ba^{2+} to the bath solution, while residual outward currents remained under these conditions. The Ba^{2+} sensitive currents (c) were isolated when the Ba^{2+} resistant currents were subtracted from the corresponding control traces. **d:** To quantitatively estimate the portion of inward rectifier currents, the passive component (determined as described in the legend to Fig. 4c) was subtracted from the whole membrane current, and g_{IR} was subsequently calculated at −130 mV. Finally, g_{IR} was divided by the maximum outward conductivity, g_{out}, activated at 20 mV (see inset in d). This ratio was compared during development, demonstrating a significant increase in the relative contribution of g_{IR} after p9. Data were determined from at least 7 and at most 28 cells; 1 μM TTX was added to block voltage operated Na^+ channels.

medium and in cocultures containing neurons (Thio et al., 1993). The mechanisms and the physiological significance of glial Na^+ channel down-regulation have not yet been elucidated. In immature neurons, an increase in intracellular Na^+ was shown to induce a decrease in Na^+ channel density by channel internalization, but this mechanism does not seem to be operative in cultured astrocytes (Dargent and Couraud, 1990; Dargent et al., 1994).

Changes in K^+ Currents During Maturation

We could separate four different types of K^+ currents in the "complex" hippocampal glial cells. Up to p9, the current pattern was clearly dominated by transient and sustained outward K^+ currents with the latter mainly comprising delayed rectifier currents. Pharmacological, kinetic, and stationary properties of these two components were previously quantified at a given age (Jabs et al., 1994; Steinhäuser et al., 1994b). Here we show that these properties significantly changed during ontogenesis. The sensitivity of I_A to 4-AP was considerably less at p5 as compared to all later age groups analyzed (Table 2). Such changes were not observed in the nearby CA1 pyramidal neurons (Spigelman et al., 1992), but in granule cells of the dentate gyrus (Beck et al., 1992), very similar variations were found as in the glial cells of the stratum radiatum. In the latter study, it was speculated that these variable pharmacological characteristics of I_A could be due to changes in the lipid environment of K^+ channels observed during ontogenesis. Besides these different age-dependent pharmacological properties, we also detected changes in the kinetics of I_A, with the time constants of activation and inactivation significantly increasing between p10 and p20. While the ratio g_A/g_K remained unchanged in p5–9 cells, in older cells, the transient conductance exceeded the delayed rectifier by far. This is in contrast to the regula-

tion of I_A and I_K in neurons of the hippocampus where different sustained K^+ currents were reported to develop only at later stages of development (Beck et al., 1992; Spigelman et al., 1992); astrocytes were found to modulate the appearance of transient neuronal K^+ currents in the hippocampal cell culture (Wu and Barish, 1994).

After p20, the current pattern of the "complex" glial cells changed considerably. An increasing time- and voltage-independent passive K^+ conductance appeared, which now dominated the sustained outward currents and by far exceeded I_K and I_A. In addition, the older cells expressed inward rectifier currents. Since g_P and g_{IR} were selectively permeable to K^+ ions and were active at rest, these conductances mainly establish the resting potential and stabilize it close to E_K. The properties of I_{IR} and its delayed expression in the "complex" cells resembled findings on astrocytes in other preparations (Barres et al., 1990; Glassmeier et al., 1994; Ransom and Sontheimer, 1995; Sontheimer et al., 1992; Tse et al., 1992). In addition, we observed an enhanced portion of dye coupling at p30, but still the majority of "complex" cells failed to be coupled. A similar low percentage of astroglial coupling was observed in the cell culture (Sontheimer et al., 1991b). It should be noted that the large increase in passive currents was not predominantly mediated by junctional currents because halothane only slightly reduced the current amplitudes and in particular because large passive currents were preserved in glial cells acutely isolated from the CA1 stratum radiatum (Seifert and Steinhäuser, 1995). However, it is possible that we underestimated the portion of coupled cells because LY does not seem to be an optimal marker for the detection of astrocytic gap junctions in the juvenile hippocampus (Konietzko and Müller, 1994). The shift in channel expression reported here is not unique for astrocytes because a very similar "replacement" of voltage gated Na^+ and K^+ outward currents by passive and inward rectifier K^+ currents occurs during development of oligodendrocytes from their precursor cells (Berger et al., 1991, 1992; Sontheimer et al., 1989).

There is no doubt that glial cells of different developmental stages coexist in the CA1 stratum radiatum and probably also in other areas of the juvenile CNS, which gives rise to a heterogeneity in electrophysiological properties of cells characterized in situ at a given age (Berger et al., 1991, 1992; Müller et al., 1994; Sontheimer and Waxman, 1993; Steinhäuser et al., 1992, 1994a). In the present study, we met a few "complex" cells possessing noticeable passive currents even at p5, the earliest age analyzed. In addition, some cells of the p9 group already expressed inward rectifier currents. After p20, however we never found a cell with negligible g_P and g_{IR}, i.e., properties which typically characterized the p5 cells. One can therefore speculate that "passive" cells represent a final, mature stage of ion channel phenotype in situ. This idea is also supported by our immunocytochemical data because positive staining for GFAP, a marker that recognizes mature astrocytes, was only observed in cells which predominantly expressed the passive K^+ conductance (see also Steinhäuser et al., 1994a).

Functional Implications

Glial cells are thought to participate in the regulation of extracellular K^+ concentrations in the neuronal microenvironment by spatial buffering (Orkand et al., 1966) and K^+ siphoning via the activation of inward rectifier channels (Brew et al., 1986; Newman et al., 1984). The present study shows that in glial cells of the hippocampus, significant inward rectification is expressed only later in postnatal development. In addition, only with maturation did a time- and voltage-independent K^+ resting conductance appear that stabilized the glial resting potential close to E_K. These results are compatible with findings on an impaired homeostasis, and an increased readiness of the cortex to develop K^+ induced epileptiform activity early in postnatal development, which were speculated to be due to insufficient gliogenesis and glial cell function (Hablitz and Heinemann, 1987; Jendelova and Sykova, 1991; Nixdorf-Bergweiler et al., 1994). The total number of glial cells considerably increases until 30 days in the postnatal mouse neocortex (Heumann et al., 1978). In the brain of young animals, the extracellular space volume fraction amounts to about 40%, i.e., it is twice as large as in the adult brain (Lehmenkühler et al., 1993). We found the most significant changes in the glial membrane current pattern between p10 and p20, and just at the same time window, Lehmenkühler et al. (1993) observed a prominent reduction in volume fraction in the rat cortex. It is thus conceivable that in the young animals, changes in $[K^+]_o$ are buffered mainly due to dilution in the larger extracellular volume. With further development, the ECS volume decreases and these morphological changes go hand in hand with functional changes. Glial cells develop mechanisms to maintain homeostasis in the smaller extracellular space, and thus their functional properties change in response to the variable demands during brain maturation. However, the significance of voltage operated Na^+ and K^+ outward currents expressed in the immature glial cells still has to be elucidated.

ACKNOWLEDGMENTS

This research was supported by the Bundesministerium für Forschung und Technologie (grant to C.S.), Landesgraduiertenprogramm (stipend to E.K.), the Gertrud Reemtsma Foundation (stipend to R.J.), and the Sandoz Foundation (stipend to C.S.). The authors would like to thank I. Krahner for excellent technical assistance.

REFERENCES

Barres, B.A., Koroshetz, W.J., Chun, L.L.Y., and Corey, D.P. (1990) Ion channel expression by white matter glia: The type-1 astrocyte. *Neuron*, 5:527–544.

Beck, H., Ficker, E., and Heinemann, U. (1992) Properties of two voltage-activated potassium currents in acutely isolated juvenile rat dentate gyrus granule cells. *J. Neurophysiol.*, 68:2086–2099.

Berger, T., Schnitzer, J., and Kettenmann, H. (1991) Developmental changes in the membrane current pattern, K^+ buffer capacity and morphology of glial cells from the corpus callosum slice. *J. Neurosci.*, 11:3008–3024.

Berger, T., Schnitzer, J., Orkand, P.M., and Kettenmann, H. (1992) Sodium and calcium currents in glial cells of the mouse corpus callosum slice. *Eur. J. Neurosci.*, 4:1271–1284.

Blankenfeld, G. von, Verkhratsky, A.N., and Kettenmann, H. (1992) Ca^{2+} channel expression in the oligodendrocyte lineage. *Eur. J. Neurosci.*, 4:1035–1048.

Borges, K., Ohlemeyer, C., Trotter, J., and Kettenmann, H. (1994) AMPA/kainate receptor activation in murine oligodendrocyte precursor cells leads to activation of a cation conductance, calcium influx and blockade of delayed rectifying K^+ channels. *Neuroscience,* 63:135–149.

Brew, H., Gray, P.T.A., Mobbs, P., and Attwell, D. (1986) Endfeet of retinal glial cells have higher densities of ion channels that mediate K buffering. *Nature,* 324:466–468.

Brookes, N. and Turner, R.J. (1994) K^+ induced alkalinization in mouse cerebral astrocytes mediated by reversal of electrogenic Na^+-HCO_3^- cotransport. *Am. J. Physiol.*, 267 (Cell Physiol. 36):C1633–C1640.

Clark, B.A. and Mobbs, P. (1994) Voltage-gated currents in rabbit retinal astrocytes. *Eur. J. Neurosci.*, 6:1406–1414.

Cummins, T.R., Xia, Y., and Haddad, G. (1994) Functional properties of rat and human neocortical voltage-sensitive sodium currents. *J. Neurophysiol.*, 71:1052–1064.

Dargent, B. and Couraud, F. (1990) Down-regulation of voltage-dependent sodium channels initiated by sodium influx in developing neurons. *Proc. Natl. Acad. Sci. U.S.A.*, 87:5907–5911.

Dargent, B., Paillart, C., Carlier, E., Alcaraz, G., Martin-Eauclaire, M.F., and Couraud, F. (1994) Sodium channel internalization in developing neurons. *Neuron,* 13:683–690.

Dermitzel, R., Hertzberg, E.L., Kessler, J.A., and Spray, D.C. (1991) Gap junctions between cultured astrocytes: Immunocytochemical, molecular, and electrophysiological aspects. *J. Neurosci.*, 11:1421–1432.

Edwards, F.A., Konnerth, A., Sakmann, B., and Takahashi, T. (1989) A thin slice preparation for patch-clamp recordings from neurones of the mammalian central nervous system. *Pflugers Arch.*, 414:600–612.

Eng, L.F. (1985) Glial fibrillary acidic protein (GFAP): the major protein of glial intermediate filaments in differentiated astrocytes. *J. Neuroimmunol.*, 8:203–214.

Gautron, S., dos Santos, G., Pinto-Henrique, D., Koulakoff, A., Gros, F., and Berwald-Netter, Y. (1992) The glial voltage-gated sodium channel: Cell- and tissue-specific mRNA expression. *Proc. Natl. Acad. Sci. U.S.A.*, 89:7272–7276.

Glassmeier, G., Jeserich, G., and Krüppel, T. (1994) Voltage-dependent sodium and potassium currents in cultured trout astrocytes. *Glia,* 11:245–254.

Hablitz, J.J. and Heinemann, U. (1987) Extracellular K^+ and Ca^{2+} changes during epileptiform discharges in the immature rat neocortex. *Dev. Brain Res.*, 36:299–303.

Heumann, D., Leuba, G., and Rabinowicz, T. (1978) Postnatal development of the mouse cerebral neocortex. IV. Evolution of the total cortical volume, of the population of neurons and glial cells. *J. Hirnforsch.*, 19:385–393.

Jabs, R., Kirchhoff, F., Kettenmann, H., and Steinhäuser, C. (1994) Kainate activates Ca^{2+}-permeable glutamate receptors and blocks voltage-gated K^+ currents in glial cells of mouse hippocampal slices. *Pflugers Arch.*, 426:310–319.

Jendelova, P. and Sykova, E. (1991) Role of glia in K^+ and pH homeostasis in the neonatal rat spinal cord. *Glia,* 4:56–63.

Kettenmann, H. and Ransom, B. (1988) Electrical coupling between astrocytes and between oligodendrocytes studied in mammalian cell cultures. *Glia,* 1:64–73.

Konietzko, U. and Müller, C.M. (1994) Astrocytic dye coupling in rat hippocampus: topography, developmental onset, and modulation by protein kinase C. *Hippocampus,* 4:297–306.

Kressin, K., Kuprijanova, E., and Steinhäuser, C. (1994) Properties of K^+ and Na^+ currents in mouse hippocampal glial cells during development. *Eur. J. Neurosci.*, S7:55.

Landry, C.F., Ivy, G.O., and Brown, I.R. (1990) Developmental expression of glial fibrillary acidic protein mRNA in the rat brain analyzed by in situ hybridization. *J. Neurosci. Res.*, 25:194–203.

Lehmenkühler, A., Sykova, E., Svoboda, J., Zilles, K., and Nicholson, C. (1993) Extracellular space parameters in the rat neocortex and subcortical white matter during postnatal development determined by diffusion analysis. *Neuroscience,* 55:339–351.

Minkwitz, H.-G. (1976) Zur Entwicklung der Neuronenstruktur des Hippocampus während der prä- und postnatalen Ontogenese der Albinoratte. II. Mitteilung: Neurohistologische Mitteilung: Darstellung der En-wicklung von Interneuronen und des Zusammenhanges lang-und kurzaxoniger Neurone. *J. Hirnforsch.*, 17:233–253.

Minturn, J.E., Sontheimer, H., Black, J.A., and Waxman, S.G. (1992) Sodium channel expression in optic nerve astrocytes chronically deprived of axonal contact. *Glia,* 6:19–29.

Müller, T., Fritschy, J.M., Grosche, J., Pratt, G.D., Möhler, H. and Kettenmann, H. (1994) Developmental regulation of voltage-gated K^+ channel and $GABA_A$ receptor expression in Bergmann glial cells. *J. Neurosci.*, 14:2503–2514.

Newman, E.A., Frambach, D.A., and Odette, L.L. (1984) Control of extracellular potassium levels by retinal glial cell siphoning. *Science,* 225:1174–1175.

Nixdorf-Bergweiler, B.E., Albrecht, D., and Heinemann, U. (1994) Developmental changes in the number, size, and orientation of GFAP-positive cells in the CA1 region of rat hippocampus. *Glia,* 12:180–195.

O'Connor, E.R., Sontheimer, H., and B.R. Ransom (1994) Rat hippocampal astrocytes exhibit electrogenic sodium-bicarbonate co-transport. *J. Neurophysiol.*, 72:2580–2588.

Orkand, R.K., Nicholls, J.G., and Kuffler, S.W. (1966) Effect of nerve impulses on the membrane potential of glial cells in the central nervous system of amphibia. *J. Neurophysiol.*, 29:788–806.

Patel, A.J. (1986) Development of astrocytes: In vivo and in vitro studies. *Adv. Biosci.*, 61:87–96.

Ransom, B.R. and Kettenmann, H. (1990) Electrical coupling, without dye coupling, between mammalian astrocytes and oligodendrocytes in cell culture. *Glia,* 3:258–266.

Ransom, C.B. and Sontheimer, H. (1995) Biophysical and pharmacological characterization of inwardly rectifying K^+ currents in rat spinal cord astrocytes. *J. Neurophysiol.*, 73:333–346.

Ritchie, J.M. (1992) Voltage-gated ion channels in schwann cells and glia. *Trends Neurosci.*, 15:345–351.

Sah, P., Gibb, A.J., and Gage, P.W. (1988) The sodium current underlying action potentials in guinea pig hippocampal CA1 neurons. *J. Gen. Physiol.*, 91:373–398.

Sakmann, B. and Trube, G. (1984) Conductance properties of single inwardly rectifying potassium channels in ventricular cells from guinea-pig heart. *J. Physiol. (Lond.),* 347:641–657.

Schütz, H., Stutter, E., Weller, K., and Petri, I. (1984) Design and data analysis on DNA-binding experiments. *Stud. Biophys.*, 104:23–34.

Schwartzkroin, P.A. and Mathers, L.H. (1978) Physiological and morphological identification of a nonpyramidal hippocampal cell type. *Brain Res.*, 157:1–10.

Seifert, G. and Steinhäuser, C. (1995) Glial cells in the mouse hippocampus express AMPA receptors with an intermediate Ca^{2+} permeability. *Eur. J. Neurosci.*, in press.

Seifert, G., Kuprijanova, E., Steinhäuser, C., Krämer, A., Lang, E., Reinhardt, S., and Maelicke, A. (1995) Immunocytochemical identification of early astrocytes in the juvenile mouse hippocampus. In: *Proceedings of the 23rd Göttingen Neurobiology Conference.* Elsner, N. and Menzel, R. (eds.), G. Thieme Verlag, Stuttgart, p. 176.

Sommer, I. and Schachner, M. (1981) Monoclonal antibodies (O1 to O4) to oligodendrocyte cell surfaces: An immunocytological study in the central nervous system. *Dev. Biol.*, 83:311–327.

Sontheimer, H., Trotter, J., Schachner, M., and Kettenmann, H. (1989) Channel expression correlates with differentiation stage during the development of oligodendrocytes from their precursor cells in culture. *Neuron,* 2:1135–1145.

Sontheimer, H., Ransom, B.R., Cornell-Bell, H., Black, J.A., and Waxman, S.G. (1991a) Na^+-current expression in rat hippocampal astrocytes in vitro: alterations during development. *J. Neurophysiol.*, 65:3–19.

Sontheimer, H., Waxman, S.G., and Ransom, B.R. (1991b) Relationship between Na^+ current expression and cell-cell coupling in astrocytes cultured from rat hippocampus. *J. Neurophysiol.*, 65:989–1002.

Sontheimer H., Black, J.A., Ransom, B.R., and Waxman, S.G. (1992) Ion channels in spinal cord astrocytes in vitro. I. Transient expression of high levels of Na^+ and K^+ channel. *J. Neurophysiol.*, 68:985–1000.

Sontheimer, H. and Waxman, S.G. (1993) Expression of voltage-activated ion channels by astrocytes and oligodendrocytes in the hippocampal slice. *J. Neurophysiol.*, 70:1863–1873.

Sontheimer, H. (1994) Voltage-dependent ion channels in glial cells. *Glia,* 11:156–172.

Spigelman, I., Zhang, L., and Carlen, P.L. (1992) Patch-clamp study of postnatal development of CA1 neurons in rat hippocampal slices: Membrane excitability and K^+ currents. *J. Neurophysiol.*, 68:55–69.

Spitzer, N.C. (1991) A developmental handshake: Neuronal control of ionic currents and their control of neuronal differentiation. *J. Neurobiol.*, 22:659–673.

Steinhäuser, C., Tennigkeit, M., Matthies, H., and Gündel, J. (1990) Properties of the fast sodium channels in pyramidal neurones iso-

lated from the CA_1 and CA_3 areas of the hippocampus. *Pflugers Arch.*, 415:756–761.
Steinhäuser, C., Berger, T., Frotscher, M., and Kettenmann, H. (1992) Heterogeneity in the membrane current pattern of identified glial cells in the hippocampal slice. *Eur. J. Neurosci.*, 4:472–484.
Steinhäuser, C. (1993) Electrophysiological characteristic of glial cells. *Hippocampus*, 3:S113–124.
Steinhäuser, C., Jabs, R., and Kettenmann, H. (1994a) GABA and glutamate responses in identified glial cells of the mouse hippocampal slice. *Hippocampus*, 4:16–39.
Steinhäuser, C., Kressin, K., Kuprijanova, E., Weber, M., and Seifert, G. (1994b) Properties of voltage-activated sodium and potassium currents in mouse hippocampal glial cells in situ and after acute isolation from tissue slices. *Pflugers Arch.*, 428:610–620.
Thio, C.L., Waxman, S.G., and Sontheimer, H. (1993) Ion channels in spinal cord astrocytes in vitro. III. Modulations of channel expression by coculture with neurons and neuron-conditioned medium. *J. Neurophysiol.*, 69:819–831.
Tse, F.W., Fraser, D.D., Duffy, S., and MacVicar, B.A. (1992) Voltage-activated K^+ currents in acutely isolated hippocampal astrocytes. *J. Neurosci.*, 12:1781–1788.
Walz, W. (1989) Role of glial cells in the regulation of the brain ion microenvironment. *Prog. Neurobiol.*, 33:309–333.
Wilkin, G.P., Marriot, E.R., and Cholewinski, A.J. (1990) Astrocyte heterogeneity. *Trends Neurosci.*, 13:43–46.
Williams, S., Samulack, D.D, Beaulieu, C., and Lacaille, J.C. (1994) Membrane Properties and synaptic responses of interneurons located near the stratum lacunosum-moleculare/radiatum border of area CA1 in whole-cell recordings from rat hippocampal slices. *J. Neurophysiol.*, 71:2217–2235.
Wu, R.-L and Barish, M.E. (1994) Astroglial modulation of transient potassium current development in cultured mouse hippocampal neurons. *J. Neurosci.*, 14:1677–1687.
Xia, Y. and Haddad, G. (1994) Postnatal development of voltage-sensitive Na^+ channels in rat brain. *J. Comp. Neurol.*, 345:279–287.